https://doi.org/10.5194/soil-2021-45
Preprint. Discussion started: 27 May 2021

SOIL Discussions Open Access EGU

Biochar alters hydraulic conductivity and inhibits nutrient leaching in two agricultural soils

Danielle L. Gelardi[1], Irfan Ainuddin[2], Devin A. Rippner[3], Majdi Abou Najm[1], Sanjai J. Parikh[1]

[1]Land, Air and Water Resources, University of California, Davis, 1 Shields Ave, Davis CA 95616, USA
[2]California State University Chico, 400 West First Street, Chico, CA, 95929, USA
[3]United States Department of Agriculture, Horticulture Crops Research Unit, Davis, Prosser, WA

Correspondence to: Danielle L. Gelardi (dlgelardi@ucdavis.edu)

Abstract. Biochar is purported to provide agricultural benefits when added to the soil, through changes in soil water hydraulic conductivity (K_{sat}), and increased nutrient retention through chemical or physical means. Despite increased interest and investigation, there remains uncertainty regarding the ability of biochar to deliver these agronomic benefits due to differences in biochar feedstock, production method, production temperature and soil texture. In this project, a suite of experiments was carried out using biochars of diverse feedstocks and production temperatures, in order to determine the biochar parameters which may optimize agricultural benefits. Sorption experiments were performed with seven distinct biochars to determine sorption efficiencies for ammonium and nitrate. Only one biochar effectively retained nitrate, while all biochars bound ammonium. The three biochars with the highest binding capacities (produced from almond shell at 500 and 800 °C (AS500 and AS800) and softwood at 500 °C (SW500)) were chosen for column experiments. Biochars were amended to a sandy loam and a silt loam at 0 and 2% (w/w) and saturated hydraulic conductivity (K_{sat}) was measured. Biochars reduced K_{sat} in both soils by 64-80%, with the exception of AS800, which increased K_{sat} by 98% in the silt loam. Breakthrough curves for nitrate and ammonium, as well as leachate nutrient concentration, were also measured in the sandy loam columns. All biochars significantly decreased the quantity of ammonium in the leachate, by 22 to 78%, and slowed its movement through the soil profile. Ammonium retention was linked to high cation exchange capacity and a high oxygen to carbon ratio, indicating that the primary control of ammonium retention in biochar-amended soils is the chemical affinity between biochar surfaces and ammonium. Biochars had little to no effect on the timing of nitrate release, and only SW500 decreased total quantity, by 27 to 36%. The ability of biochar to retain nitrate may be linked to high surface area, suggesting a physical entrapment rather than a chemical binding. Together, this work sheds new light on the combined chemical and physical means by which biochar may alter soils to impact nutrient leaching and hydraulic conductivity for agricultural production.

https://doi.org/10.5194/soil-2021-45
Preprint. Discussion started: 27 May 2021

1 Introduction

The ability of biochar to chemically and physically alter soil environments for specific agronomic benefits is the subject of increased investigation, as evidenced by the recent rise in published biochar studies (Web of Science, 2020) and United States trademark and patent applications listing the word "biochar" (US Patent and Trademark Office, 2021). Biochar, or the carbonaceous material created from the thermochemical conversion of biomass in an oxygen-limited environment (International Biochar Initiative (IBI), 2015), possesses unique chemical and physical properties, determined by variables such as its feedstock, production method, and production temperature. Biochar properties typically include a low bulk density, high porosity, high surface area, reactive surface functional groups, and recalcitrant carbon (Downie et al., 2009). These attributes make it a promising material for amendment to agricultural soils, as biochar may help improve soil water holding capacity, hydraulic conductivity, and nutrient retention. Despite increased interest and investigation, there remains uncertainty regarding the ability of biochar to deliver these agronomic benefits. While many studies show promising results where nutrient retention and soil water dynamics are concerned (Blanco-Canqui, 2017; Glaser et al., 2002, 2015; Glaser and Lehr, 2019; Haider et al., 2020; Hestrin et al., 2019), others have demonstrated no or only minor effects (Griffin et al., 2017; Jones et al., 2012; Martos et al., 2020). Several authors have concluded that, due to differences in biochar production parameters and those of the soil environment, material and site-specific investigation is required before conclusions can be drawn about the potential of biochar to provide agricultural benefits (Hassan et al., 2020; Jeffery et al., 2011; Zhang et al., 2016).

The ability of biochar to remove nitrate and ammonium from aqueous environments has been widely investigated, as it may indicate whether biochar can improve crop nutrient use efficiency and supress fertilizer pollution through leaching and volatilization. To this effect, batch sorption experiments are commonly carried out to determine the electrostatic affinity between biochars and nitrate and ammonium. Due to the deprotonation of surface functional groups at agronomic soil pHs, biochar is typically negatively charged. It is expected, then, that it would not bind to nitrate, which exists in the anionic form in aqueous environments. Electrostatic repulsion between nitrate and biochar has indeed been regularly cited as the reason behind little to no nitrate removal in batch sorption experiments. Zhou et al. (2019) tested biochars from four feedstocks, each produced at three temperatures, to find minimal nitrate sorption or even nitrate release. Similarly, Sanford et al. (2019) found that five biochars from diverse feedstocks and production temperatures had zero nitrate binding capacity. Little to no nitrate sorption capacity has been commonly observed for biochars produced from a broad range of feedstocks, productions methods, and temperatures (Gai et al., 2014b; Hale et al., 2013a; Hollister et al., 2013; Li et al., 2018; Wang et al., 2017; Zeng et al., 2013). Though exceptions have been observed in which biochars exhibited high nitrate binding capacities (Ahmadvand et al., 2018; Chandra et al., 2020), a recent study determined the average published maximum adsorption capacity (Q_{max}) of unmodified biochar for NO_3-N to be as low as 1.95 mg g^{-1} (Zhang et al., 2020).

This same study determined the average published Q_{max} of unmodified biochar for NH_4^+-N to be 11.19 mg g^{-1} (Zhang et al., 2020). Higher Q_{max} values for biochar and ammonium are to be expected, as ammonium exists in the cationic form in aqueous environments and would more readily adsorb to negatively charged biochar surfaces. While this theoretical electrostatic

https://doi.org/10.5194/soil-2021-45
Preprint. Discussion started: 27 May 2021

affinity is supported by higher Q_{max} values throughout published sorption experiments, inconsistencies can still be found. Q_{max} values lower than 2 mg NH_4^+ g^{-1} are commonly observed, for biochars produced from a broad range of temperatures and feedstocks (Hale et al., 2013b; Paramashivam et al., 2016; Song et al., 2019; Tian et al., 2016; Uttran et al., 2018; Wang et al., 2015; Yin et al., 2019; Zhang et al., 2017). While most reported Q_{max} values are less than 20 mg NH_4^+-N g^{-1} (Zhang et al., 2020), values as high as 93.6 mg NH_4^+ g^{-1} (Yin et al., 2018) and 243.3 mg NH_4^+ g^{-1} have been observed (Gao et al., 2015). Biochars exhibit a broad range of ammonium sorption capacities and conflicting trends have emerged. Multiple authors have observed that sorption capacity decreases with increasing production temperature (Gai et al., 2014a; Gao et al., 2015; Yin et al., 2018). Lower temperatures have been correlated with higher cation exchange capacity (CEC) (Gai et al., 2014a), and higher O/C ratios (Yang et al., 2017). These properties may contribute to biochars with the ability to remove ammonium from solution, as they provide a greater number of exchange sites and oxygen-containing functional groups which can react with ammonium (Yang et al., 2017). The reverse trend has also been observed, however, with authors noting that an increase in production temperature resulted in higher ammonium Q_{max} values (Chandra et al., 2020; Zeng et al., 2013; Zheng et al., 2013). These authors point towards the higher specific surface area (SA) of biochar at higher production temperatures as a critical parameter to predicting ammonium adsorption.

Chemical bonding and electrostatic interactions may not be the only mechanism by which biochar retains nitrate and ammonium in soils. Despite the lack of chemical affinity between nitrate and biochar, studies frequently demonstrate the ability of biochar to reduce nitrate leaching in soil column studies and pot trials (Haider et al., 2016; Kameyama et al., 2012; Pratiwi et al., 2016; Yao et al., 2012). While some authors hypothesize the mechanism to be microbial immobilization (Bu et al., 2017), others have found the addition of biochar to stimulate N mineralization (Teutscherova et al., 2018). In addition to chemical and microbial mechanisms, biochar may retain N through physical means (Clough and Condron, 2010). One study determined that biochar decreased soil bulk density by 3 to 31%, and increased porosity by 14 to 64% (Blanco-Canqui, 2017). Biochar can also alter mean pore size and pore architecture, thereby influencing tortuosity and the residence time of water and nutrients within the soil profile (Lim et al., 2016; Quin et al., 2014). The impact of biochar on hydraulic conductivity largely appears dependent on soil texture, which highly influences pore structure. While exceptions have been observed, biochar has largely been shown to decrease the ability of a saturated soil to transmit water (saturated hydraulic conductivity (K_{sat})) in coarse textured soils and increase K_{sat} in finer soils (Blanco-Canqui, 2017). The impact of biochar on these soil physical properties may influence nitrate retention through a mechanism known as “nitrate capture,” in which nitrate molecules become physically entrapped within biochar pores (Haider et al., 2016), potentially leading to increased residence time in crop rooting zones and a greater opportunity for plant uptake (Haider et al., 2020; Kameyama et al., 2012; Kammann et al., 2015).

In this project, a suite of experiments was carried out using biochars of diverse feedstocks and production temperatures, in order to determine to what degree these biochars: 1) chemically bind nitrate and ammonium; 2) physically alter the soil to influence saturated hydraulic conductivity; or 3) influence nutrient leaching, through either chemical or physical means. This information was used to determine the soil and biochar parameters which may optimize hydrologic and nutrient retention benefits in two agricultural soils, and to investigate the combination of chemical and physical mechanisms by which these

https://doi.org/10.5194/soil-2021-45
Preprint. Discussion started: 27 May 2021

benefits are delivered. Sorption experiments were performed with seven distinct, commercially available biochars to determine nutrient removal efficiencies for ammonium and nitrate. Due to their high sorption capacities, almond shell biochars produced at 500 and 800 °C (AS500 and AS800) and softwood at 500 °C (SW500) were selected for a series of soil column experiments. These biochars were amended to a sandy loam and a silt loam at 0 and 2% (w/w) and K_{sat} was measured. Breakthrough curves for nitrate and ammonium, as well as leachate nutrient concentrations, were also determined in the sandy loam columns. Together, these data elucidate the combination of chemical and physical means by which biochar impacts nutrient leaching and hydraulic conductivity. Data can be used to inform the production or modification of biochars for these specific purposes, as well as for predicting how biochars may behave in specific agricultural conditions.

2 Materials and methods

2.1 Biochar characterization

Seven biochars from four commercial companies were obtained from the following feedstocks and produced at the following temperatures: almond shell at 500 and 800 °C (AS500, AS800), coconut shell at 650 °C (CS650), softwood at 500, 650, and 800 °C (SW500, SW650, SW800), and an additional softwood biochar produced at 500 °C and inoculated with a microbial formula (SW500-I). Unless otherwise stated, biochars were sieved to 2 mm and characterized using procedures recommended by the International Biochar Initiative (IBI, 2015): pH and electrical conductivity (EC) were measured at a 1:20 biochar to 18.2 MΩ-cm water (Barnstead nanopore, Thermo Fisher) dilution (w:v) after solutions were shaken for 90 minutes; total carbon, nitrogen, hydrogen, and oxygen were measured using a dry combustion-elemental analyzer (Costech ECS4010); and moisture, volatile, and ash content were measured as a percent of total dry weight through sequential increases in furnace temperature (105, 750, and 950 °C, respectively). Particle size distribution was measured by laser diffraction (Coulter LS230). CEC was measured using a combination of the modified ammonium acetate compulsory displacement method (Gaskin et al., 2008) and the rapid saturation method (Mukome et al., 2013; Mulvaney et al., 2004): 0.25g of biochar was leached with 18.2 MΩ-cm water (w:v) under vacuum (-20 to -40 kPa). Leachate was stored and analyzed for dissolved organic carbon (DOC) through combustion (Shimadzu TOC-V). Biochar samples were then washed with 1 M sodium acetate (pH 8.2) until the EC of the elute was the same as the eluant. Samples were rinsed three times with 10 ml of 2-proponal, then dried under vacuum for 10 minutes. To displace sodium ions, biochars were washed with 1 M ammonium acetate in same volume as was required sodium acetate. Leachate was collected and analyzed for sodium concentration through atomic absorption spectroscopy (Perkin Elmer AAnalyst 800).

Specific surface area was determined by Micromeritics' Particle Testing Authority (https://www.particletesting.com/) from CO_2 adsorption isotherms according to the Brunauer, Emmet, Teller (BET) method (ISO [International Organization for Standardization], 2010). Fourier transform infrared (FTIR) spectra of AS500, AS800, and SW500 biochars were collected using diffuse reflectance infrared Fourier transform spectroscopy (DRIFT; PIKE Technologies EasiDiff) with air dried samples

https://doi.org/10.5194/soil-2021-45
Preprint. Discussion started: 27 May 2021

diluted to 3% with potassium bromide. All FTIR spectra were collected using a Thermo Nicolet 6700 FTIR spectrometer (Thermo Scientific) using 256 scans, 4 cm^{-1} resolution, and a DTGS detector. FTIR bands were assigned as in Parikh et al. (2014). Gross morphological differences among AS500, AS800, and SW500 were visualized by X-ray micro-computed tomography (X-ray microCT) at the Lawrence Berkeley National Laboratory Advance Light Source on beamline 8.3.2, using a beam energy of 21 KeV. Biochars were sieved to 2mm and mounted in syringes of 8.3mm diameter for imaging. A total of 1025 projections were acquired using continuous tomography mode with a 4x objective, for a final pixel size of 1.7 µm. Images were reconstructed using Gridrec methods via TomoPy and Xi-CAM (Gürsoy et al., 2014; Pandolfi et al., 2018). Image analysis was completed in Dragonfly, a 3D image analysis software free for non-commercial use (Object Research Systems, Canada).

2.2 Soil characterization

Hanford sandy loam (HSL) and Yolo silt loam (YSiL) soils were chosen for continuity between laboratory experiments and ongoing field trials. Collectively, these soils represent over 260,000 hectares of arable land in California and offer textural distinctions within a range of soils commonly farmed in the Central Valley of California (Soil Survey Staff, 2014). Soils were located via Web Soil Survey (http://websoilsurvey.sc.egov.usda.gov/) and collected from the top 30 cm in fallowed agricultural fields in Parlier, California (HSL) and Davis, California (YSiL). Soils were homogenized and sieved to 2 mm for characterization and column experiments. Colorimetric NO_3^- and NH_4^+ measurements were made according to Doane and Horwath (2003) and Verdouw et al. (1978) (Shimadzu UV-1280). Extractable P was measured using the Olsen sodium bicarbonate extraction (Watanabe and Olsen, 1965). Concentrations of potassium, calcium, magnesium, and sodium were measured by extracting 4 g of soil with 40 ml of 1 M ammonium acetate on a shaker for 30 minutes. Nutrient concentrations of filtered extracts were determined through atomic absorption spectroscopy (Perkin Elmer AAnalyst 800). Total porosity was calculated as the pore volume divided by the total soil volume in representative cores. Pore volume was determined as the difference in weight between saturated and oven-dried (105 °C for 24 h) cores. The pH and EC of soils with and without biochar were measured via 1:2 soil to 18.2 MΩ-cm water (w:v) dilution, after 15 minutes on the shaker and 60 minutes at rest (Thomas, 1996). Soil texture analysis was performed by the Analytical Lab at the University of California, Davis (Davis, CA, USA) using the hydrometer method (Sheldrick and Wang, 1993).

2.3 Sorption experiments

To investigate the ability of biochar to adsorb ammonium and nitrate, 0.1 g of biochar was added to 40 ml of solution containing either 0, 50, 100, 200, 400, or 600 mg L^{-1} of NO_3^- (as KNO_3) or NH_4^+ (as NH_4Cl), along with method blanks. All solutions were prepared in 5.84 mg L^{-1} NaCl and, as in Hale et al. (2013a), spiked at 1% volume with a stock solution of 20 g L^{-1} of the

https://doi.org/10.5194/soil-2021-45
Preprint. Discussion started: 27 May 2021

bactericide sodium azide. All sorption experiments were performed in triplicate at 22 ± 1 °C. Tubes were placed on an end-over shaker at 8 rpm for 24 h. Supernatants were passed through a 0.45 µm filter and analysed for colorimetric NO_3^- and NH_4^+ (Shimadzu UV-1280) (Doane and Horwath, 2003; Verdouw et al., 1978). Single point sorbed ion concentration was determined at initial concentrations of 100 mg NO_3^- or NH_4^+ g^{-1} biochar using Eq. (1).

$$q = \frac{C_0 V_0 - C_f V_f}{m} \quad (1)$$

Here, q is the sorbed ion concentration (mg g^{-1}), C_0 and C_f are the initial and final sorbate concentrations, respectively (mg L^{-1}), V_0 and V_f are the initial and final solution volumes, respectively (L), and m is the mass of biochar (g). Multiple equations were tested to model the adsorption isotherms, with the Freundlich equation (Eq. (2)) demonstrating the best fit based on r^2 values.

$$q = K_f C_f^{\frac{1}{n}} \quad (2)$$

Here, q and C_f are the same as in equation 1, K_f is the Freundlich constant (mg g^{-1}), and $1/n$ is the degree of nonlinearity of the isotherm. Excel was used to determine the parameters for the equations. Using batch sorption results, AS500, AS800, and SW500 were selected for further experimentation.

2.4 Column experiments

To investigate the influence of biochar on saturated hydraulic conductivity (K_{sat}), constant head column experiments were performed in five replicates using the 5 station Chameleon Kit (Soilmoisture Equipment Corporation (SEC) 2816GX). SEC tempe cells were packed with soils amended with 0 and 2% (w/w) AS500, AS800, or SW500 biochars, to a bulk density of 1.34 ± 0.02 g cm^{-3}. An application rate of 2% was chosen as the midrange of those represented in similar experiments (Blanco-Canqui, 2017). Columns were saturated for 24 h before the start of each experiment. Each column was gravity-fed a solution of 11.1 mg L^{-1} $CaCl_2$ at a pressure head of 34 cm for 10 pore volumes. K_{sat} was calculated using data produced by SEC pressure transducers and PressureLogger software, which monitored head and flow over time. Columns were also used to investigate the nutrient retention and leaching in HSL amended with 0 and 2% biochar. Native soil nitrogen was flushed for 10 pore volumes with 11.1 mg L^{-1} $CaCl_2$, after which 50 mg L^{-1} of both NO_3^- and NH_4^+ (as NH_4Cl and KNO_3) was gravity-fed through columns for 15 pore volumes. Leachate was collected every 0.5 pore volumes and analysed for colorimetric NO_3^- and NH_4^+ as in sorption experiments (Doane and Horwath, 2003; Verdouw et al., 1978).

https://doi.org/10.5194/soil-2021-45
Preprint. Discussion started: 27 May 2021

2.5 Statistical analysis

All data were analysed with mixed models and two-way analysis of variance (ANOVA) in the stats and Tidyverse packages in R (R Core Team, 2020; Wickham et al., 2019). If a significant interaction between the fixed effects (biochar and soil type) was found, the effect of biochar within each soil type was analysed separately. For analysis of results, all effects with p-values < 0.05 were considered significant. P-values were generated using the emmeans package in R (Lenth, 2019) and corrected for multiple comparisons using Tukey's honestly significant difference (HSD) method. Plots were generated in R using the ggplot2 package (Wickham, 2016) and visualized as the mean plus or minus the standard error of the means.

3 Results

3.1 Biochar characterization

Biochars exhibited a broad range of chemical and physical properties depending on their production temperature and feedstock (Tables 1 and 2). Generally, increased production temperature was associated with higher ash content, pH, EC, and surface area, as well as decreased carbon, hydrogen, and DOC. These trends are consistent with those of a recent meta-analysis on temperature and biochar properties (Hassan et al., 2020). Softwood biochars produced at 500 and 800 °C had substantially higher surface areas than almond shell biochars produced at the same temperatures. All biochars contained less than 1% nitrogen, spanning from SW800 at 0.13% to CS650 at 0.79%. Almond shell biochars contained 4-6x more nitrogen than softwood biochars produced at the same temperature. Overall, AS800 possessed the most unique properties, with the lowest carbon content at 35.3%, the highest ash content at 55.4%, the highest EC at 27.2 mS cm^{-1}, and a basic pH of 10.13. Contrary to trends observed in the literature regarding high temperature biochars, AS800 had the highest O/C ratio at 0.56, and the second highest CEC at 53.77 cmolc kg^{-1} (Hassan et al., 2020). The unusual O content of AS800 suggests it may have been oxidized through exposure to air immediately after pyrolysis while still hot.

Table 1: Select chemical and physical biochar properties (n=3) ± standard error of the means

	AS500	AS800	CS650	SW500	SW500-I	SW650	SW800
Carbon (%)	65.8 ± 0.45	35.33 ± 0.25	71.23 ± 0.73	70.89 ± 0.25	63.49 ± 0.33	78.32 ± 0.41	41.76 ± 0.47
Nitrogen (%)	0.76 ± 0.01	0.55 ± 0.02	0.79 ± 0.04	0.13 ± 0.03	0.69 ± 0.01	0.29 ± 0.01	0.13 ± 0.03
Oxygen (%)	17.11 ± 0.75	26.44 ± 0.75	13.66 ± 0.64	17.07 ± 0.58	20.11 ± 0.23	10.18 ± 0.16	15.3 ± 0.88
Hydrogen (%)	3.05 ± 0.04	1.83 ± 0.02	3.23 ± 0.06	3.76 ± 0.01	3.79 ± 0.03	2.92 ± 0.07	1.48 ± 0.05
Molar O/C ratio	0.19 ± 0.01	0.56 ± 0.01	0.15 ± 0.01	0.18 ± 0.01	0.24 ± 0	0.1 ± 0	0.27 ± 0.01
Molar H/C ratio	0.55 ± 0.01	0.62 ± 0.01	0.54 ± 0.01	0.63 ± 0	0.71 ± 0.01	0.44 ± 0.01	0.42 ± 0.02
Volatile (%)	30.74 ± 2.67	28.17 ± 0.5	32.14 ± 0.36	37.99 ± 0.86	38.83 ± 1.21	26.87 ± 0.29	21.67 ± 0.17
Ash (%)	19.01 ± 0.99	55.35 ± 0.78	5.28 ± 0.15	4.48 ± 0.06	9.21 ± 0.53	4.45 ± 0.29	31.45 ± 1.21

https://doi.org/10.5194/soil-2021-45
Preprint. Discussion started: 27 May 2021

pH	9.34 ± 0.02	10.13 ± 0.01	7.77 ± 0.02	7.85 ± 0.02	10.43 ± 0.01	8.03 ± 0.03	10.29 ± 0.01
EC (mS cm^{-1})	3.17 ± 0.01	27.2 ± 0.12	0.28 ± 0	2.54 ± 0.02	2.05 ± 0.02	0.12 ± 0	2.71 ± 0.01
DOC (mg kg^{-1})	38322.1 ± 1776.6	1055.9 ± 52.9	644.5 ± 77.1	43776.2 ± 1103.8	32171.2 ± 934.8	423.4 ± 50.6	475.2 ± 66.9
CEC (cmolc kg^{-1})	24.02 ± 0.57	52.74 ± 0.81	26.82 ± 1.06	16.46 ± 0.39	34.13 ± 0.18	21.65 ± 0.43	60.83 ± 0.75
Mean particle size (µm)	464	269.8	609.1	493.6	241.1	212.3	139.4
Median particle size (µm)	590.6	334.8	931.2	763.5	312.8	446.3	171.2
Surface Area (m^2 g^{-1})	54.7	188.2	233.6	93.5	152.6	305.6	363.6

EC = electrical conductivity; DOC = dissolved organic carbon; CEC = cation exchange capacity

The IR spectra of AS500 and SW500 were notably similar, with carboxyl and aromatic functional groups present at 1697 and 1703 cm^{-1} (C=O) and 1410 and 1418 (COO^-); aromatic bands around 1580 cm^{-1}; C=C skeletal vibrations; out of plane C-H bending vibrations (700 to 900 cm^{-1}) associated with adjacent aromatic hydrogen bonds; and aromatic C=C and C=O stretching vibrations (1581 and 1589 cm^{-1}) (Fig. 1a, Table 2). The similarity between these biochars was expected, as each was produced at the same temperature by the same company via fractional hydropyrolysis. Additionally, the AS500 biochar included 25% softwood chips to aid the pyrolysis process. By contrast, AS800 was produced via gasification. AS800 spectra contained a strong band at 1405 cm^{-1} representing substantial contributions of COO^-, and multiple sharp IR peaks from ~1000 to 700 cm^{-1} arising from metal oxide vibrations (Fig. 1a, Table 2). The high contribution of O-rich functional groups and metal oxide vibrations is consistent with the elemental analysis of AS800, which showed high oxygen and ash content (Table 1). Each biochar was visually distinct at the macroscale (Fig. 1b). Animated reconstructions of biochar particles are provided in the supplementary information (SI) (Fig. S1a, S1b, and S1c). The macro-pores (>50 µm) of SW500 were more uniform in size compared to those of AS500 and AS800 (Fig. 1b, S1a, S1b, and S1c). The softwood chips added to the AS500 feedstock matrix are visible in the background, and contrast sharply with the almond shells (Fig. 1b and S1a). The macro-pores of AS800 appeared to increase in size (most visible in the bottom right of AS800 Fig. 1a, and in the animated reconstruction in figure S1b), due to the collapse of the lacy carbon pores that were visible in AS500 (Fig. 1b and S1a). The increase in production temperature resulted in more binomial pore size distribution in AS800, with larger macropores as well as increased quantity of micro-pores, leading to an overall increase in surface area as confirmed by BET (Table 1, Fig. 1b, SI Fig. S1b)

https://doi.org/10.5194/soil-2021-45
Preprint. Discussion started: 27 May 2021

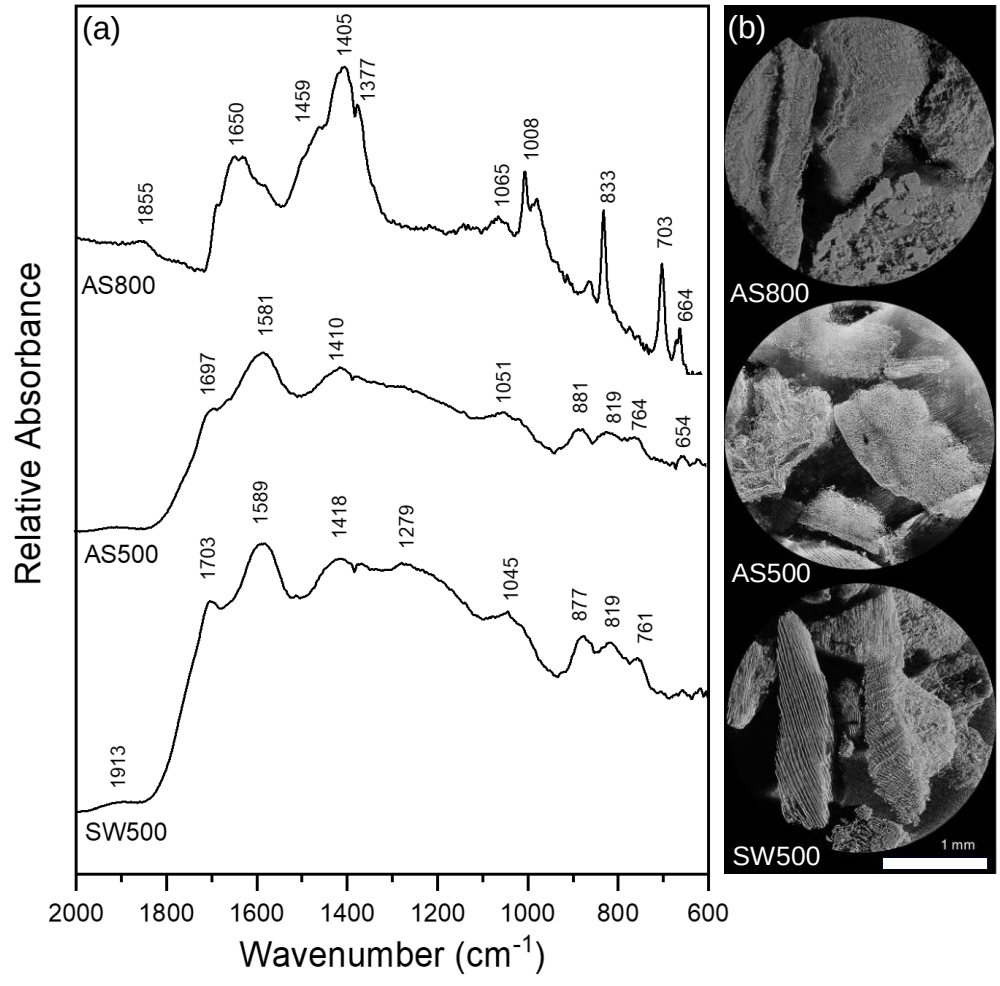

Figure 1: a) DRIFT spectra of AS800, AS500, and SW500 biochars. Samples diluted with potassium bromide to 3% sample, and collected with 256 cm^{-1} scans with a 4 cm^{-1} resolution; b) X-ray microCT images of AS800, AS500, and SW500 biochars.

230

Table 2: Functional group assignments corresponding to organic biomass

Wavenumber (cm^{-1})	Assignment*
1695-1720	v(C=O) vibration aromatic carbonyl/ carboxyl C=O stretching
1640-1660	v(C=C) vibration, C=C aromatic ring
1540-1650	v_{as}(COO)
1580-1590	Skeletal C=C vibration
1459	δ(C-H) vibrations in CH_3 and CH_2
1400-1380	v_s(COO)
1377	v(C-O) vibration aromatic and δ(C-H) vibrations in CH_3 and CH_2
1154	Aromatic C-O stretching
1080-1040	v(C-O) stretch of polysaccharides

https://doi.org/10.5194/soil-2021-45
Preprint. Discussion started: 27 May 2021

1000-1010	ν(Si-O)
870-881	1 adjacent H deformation
833	ν(metal-O)
819	2 adjacent H deformation
703	ν(metal-O)
760-765	4 adjacent H deformation
654-664	γ(OH) bend

*** FTIR band assignments from Parikh et al. (2014)**

3.2 Soil characterization

Table 3 contains select chemical and physical properties of soils used in this study. The finer textured YSiL had a porosity of 42.5%, a sand concentration of 24%, and a clay concentration of 32.7%, compared to the coarser HSL with a porosity of 29.9%, and sand and clay concentrations of 58.7%, and 12%, respectively. Both HSL and YSiL contained substantial levels of nitrate, calcium, magnesium, and potassium, and were slightly above neutral at a pH of 7.30 and 7.31, respectively.

Table 3: Select physical and chemical properties of Hanford Sandy Loam (HSL) and Yolo Silt Loam (YSiL) (n=3) ± standard error of the means

	HSL	YSiL
NH_4^+ (mg kg^{-1})	0.74 ± 0.05	1.02 ± 0.14
NO_3^- (mg kg^{-1})	34.49 ± 0.50	40.40 ± 1.05
Ca (mg kg^{-1})	943.41 ± 11.56	2191.26 ± 7.19
Mg (mg kg^{-1})	58.05 ± 1.62	508.50 ± 11.60
K (mg kg^{-1})	55.91 ± 0.99	360.05 ± 0.70
Na (mg kg^{-1})	118.09 ± 2.27	146.56 ± 0.73
Olsen P (mg kg^{-1})	9.19 ± 0.12	9.83 ± 0.15
pH	7.30 ± 0.09	7.31 ± 0.05
EC (µs cm^{-1})	427.33 ± 2.84	269.25 ± 1.92
Porosity (%)	29.9 ± 0.35	42.5 ± 0.42
Sand (%)	58.7 ± 1.4	24.0 ± 0.9
Clay (%)	12.0 ± 0.9	32.7 ± 0.5

EC = electrical conductivity

https://doi.org/10.5194/soil-2021-45
Preprint. Discussion started: 27 May 2021

3.3 Sorption

All biochars exhibited the capacity to remove ammonium from solution (Fig. 2), though K_f values were low (Table 4). Single point concentration tests at a C_0 of 100 mg L^{-1} revealed the following hierarchy of sorption capacities, in order of lowest to highest: SW650 < SW500 < CS650 < SW500-I < AS500 < SW800 < AS800 (Table 4). These q values spanned 0.70 (SW650) to 7.15 (AS800) mg g^{-1}, or removal efficiencies of 0.70 and 7.15%. AS800 exhibited the greatest K_f value at 0.16 mg NH_4^+ g^{-1}. Isotherms for nitrate and biochar are not provided, as only AS500 exhibited the capacity to remove nitrate from solution. The other six biochars released, rather than removed, nitrate. For AS500, the single point concentration test at a C_0 of 100 mg L^{-1} revealed a removal efficiency of 1.74%, or a q of 1.74 mg g^{-1} (Table 4). All tested models were poor fits for the AS500 and nitrate isotherm, including the Freundlich equation with an r^2 of 0.57. As such, K_f and 1/n values provided in Table 4 should be regarded with caution.

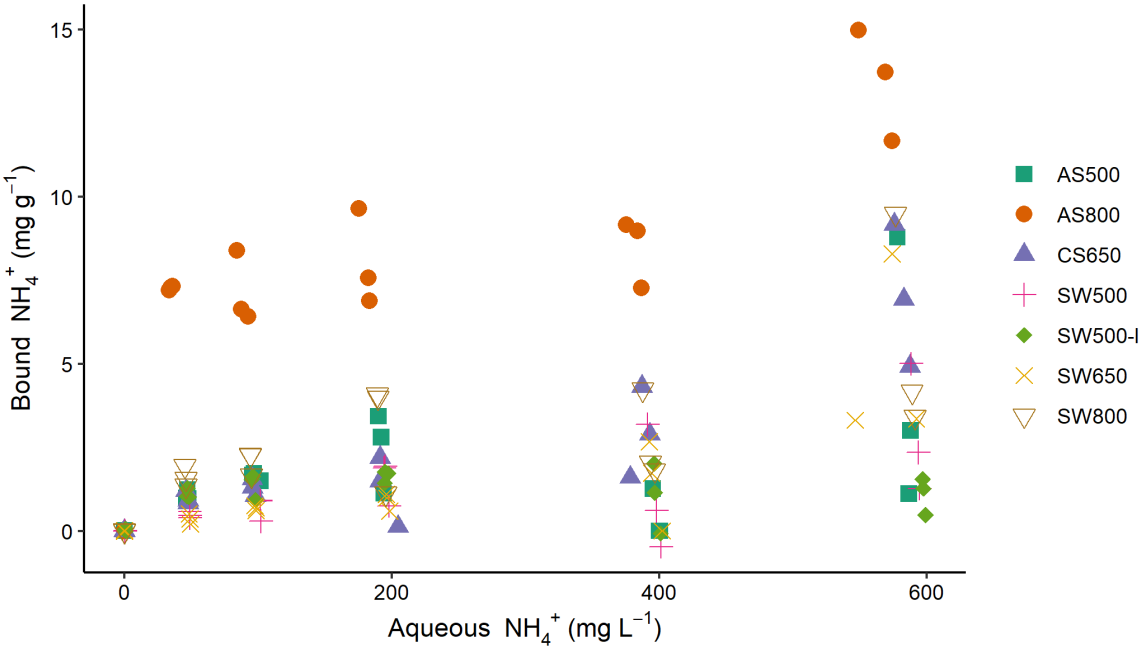

Figure 2. Sorption isotherms for ammonium and biochars, performed in at 22 ± 1 °C. All solutions were prepared in 5.84 mg L^{-1} NaCl and spiked at 1% volume with a stock solution of 20 g L^{-1} of the bactericide sodium azide.

https://doi.org/10.5194/soil-2021-45
Preprint. Discussion started: 27 May 2021

Table 4: Concentration of ions bound to biochars (mg NH_4^+ or NO_3^- g^{-1}) at single point concentration of 100 mg L^{-1}, and Freundlich model parameters (n=3). Nitrate parameters reported for only one biochar (AS500), as all other biochars released rather than removed nitrate.

	Single point concentration		Freundlich parameters		
Biochar	q (mg NH_4^+ g^{-1})	standard error	1/n	K_f (mg NH_4^+ g^{-1})	r^2
AS500	1.63	0.05	0.71	0.05	0.90
AS800	7.15	0.51	0.77	0.16	0.84
CS650	1.30	0.12	0.65	0.06	0.75
SW500	0.70	0.17	0.83	0.01	0.91
SW500-I	1.37	0.18	0.52	0.08	0.73
SW650	0.69	0.03	0.68	0.03	0.89
SW800	2.06	0.17	0.77	0.04	0.90
Biochar	q (mg NO_3^- g^{-1})	standard error	1/n	K_f (mg NO_3^- g^{-1})	r^2
AS500	1.74	0.47	0.49	0.22	0.57

3.4 Soil columns- hydraulic conductivity and breakthrough curves

There was a main effect of biochar and soil texture, as well as a significant interaction between biochar and soil texture, on saturated hydraulic conductivity ($p = 0.001$, < 0.001, and 0.006, respectively). In HSL soil, AS500 and SW500 each decreased K_{sat} by 75%, from the control at 1.2 cm s^{-1} to 0.3 cm s^{-1} ($p = 0.023$) (Fig. 3). AS800 caused a 12.5% decrease in K_{sat} to 1.05 cm s^{-1}, though the effect was not significant ($p = 0.939$). In YSiL soil, AS500 decreased K_{sat} by 63.6%, from the control at 0.044 cm s^{-1} to 0.016 ($p < 0.001$). SW500 caused a decrease of 79.5%, to 0.009 cm s^{-1} ($p < 0.001$). In contrast to its effect on HSL, AS800 increased K_{sat} in YSiL by 97.7%, to 0.087 cm s^{-1} ($p < 0.001$).

https://doi.org/10.5194/soil-2021-45
Preprint. Discussion started: 27 May 2021

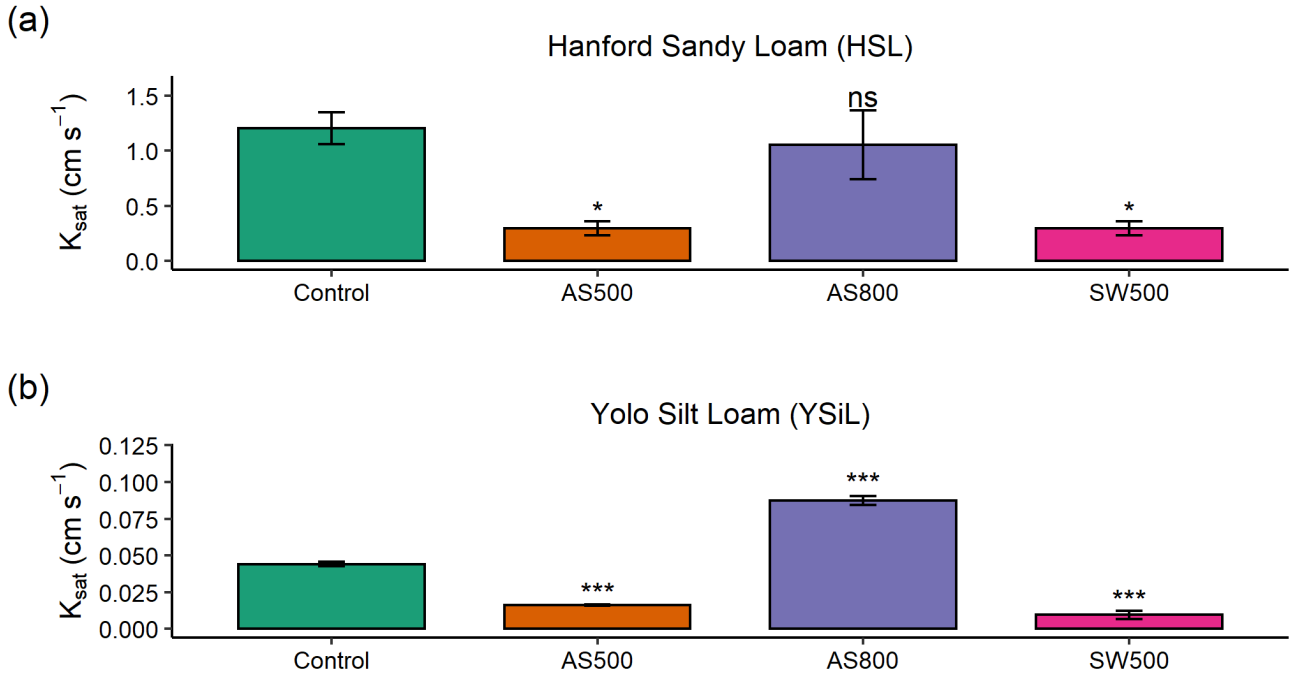

Figure 3: Impact of 0 and 2% addition of AS500, AS800, and SW500 biochars on saturated hydraulic conductivity (K_{sat}) in a) a Hanford Sandy Loam (HSL) soil and b) a Yolo Silt Loam (YSiL) soil (n=5). Symbols denote significance levels as follows: ns = not significant, *p<0.05, **p<0.01, ***p<0.001. P-values refer to comparisons between treatments and the control within each pore volume, and were corrected for multiple comparisons using Tukey's honestly significant difference method.

Figure 4 illustrates the ammonium and nitrate breakthrough curves for HSL amended with 0 and 2% AS500, AS800, and SW500. Biochar affected the timing and quantity of ammonium (introduced in pore volumes 11-25 at 50 mg L^{-1}) leached from the soil column (Fig. 4a). The estimated breakthrough point, or the pore volume at which the concentration of the leachate equals 0.5x the concentration of the incoming solution ($C/C_0 = 0.5$), was reached as follows, in order of fastest to slowest for ammonium: HSL at pore volume 14.3, SW500 at 15.5, AS500 at 16.2, and AS800 at 18.1. Biochar also significantly decreased the total amount of ammonium in the leachate at all pore volumes, as follows, in order of least to most retention: HSL < SW500 < AS500 < AS800 (Fig. 5a). At pore volume 15, AS500 decreased the ammonium concentration of the leachate compared to the control (HSL = 37.33 mg L^{-1}) by 30.5% ($p < 0.001$), AS800 by 78.1% ($p < 0.001$), and SW500 by 24.4% ($p = 0.002$). This effect was diminished by pore volume 25, where differences from the control (HSL= 41.69 mg L^{-1}) were decreased to 21.8% by AS500 ($p < 0.001$), 28.9% by AS800 ($p < 0.001$), and 8.5% by SW500 (not statistically significant at $p = 0.463$).

https://doi.org/10.5194/soil-2021-45
Preprint. Discussion started: 27 May 2021

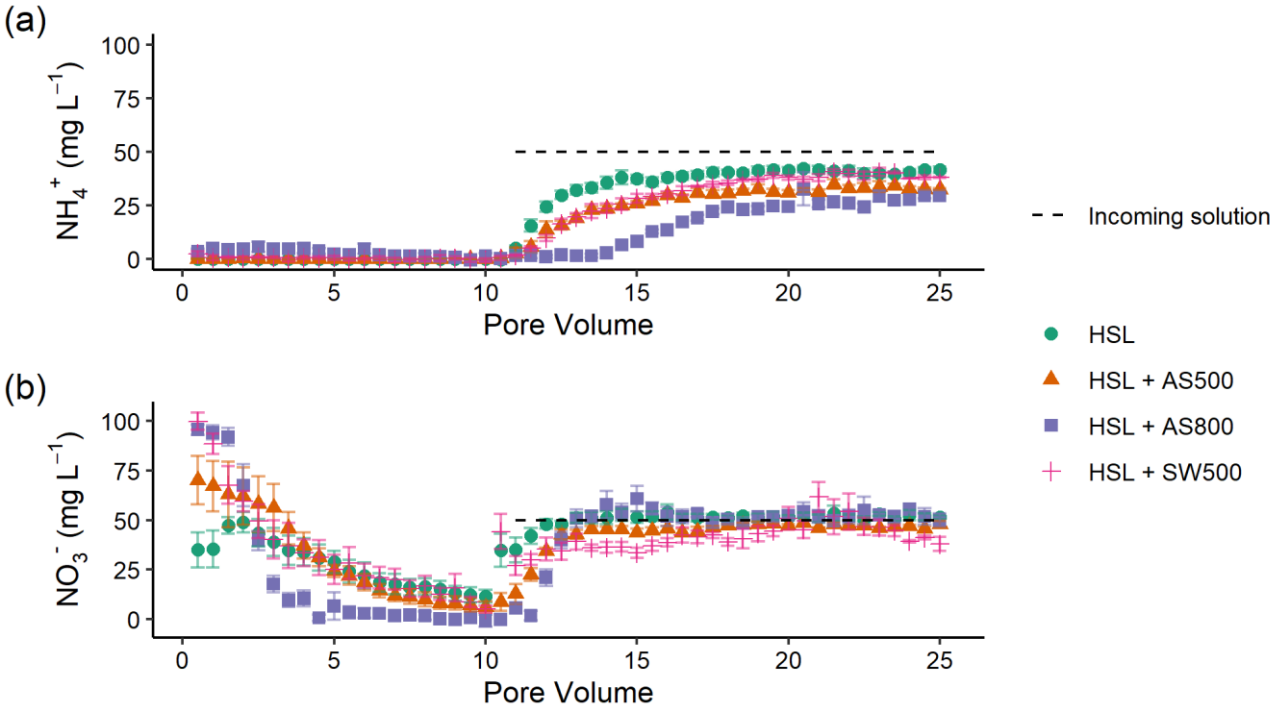

Figure 4: Breakthrough curves for a) ammonium and b) nitrate in a Handford Sandy Loam (HSL) soil with 0 and 2% additions of AS500, AS800, and SW500 biochars. Native soil nitrogen was flushed in pore volumes 0-10 with a 11.1 mg L^{-1} $CaCl_2$ solution, after which 50 mg L^{-1} solutions of NH_4^+ and NO_3^- were gravity-fed through soil columns (n=5). Error bars represent standard error of the means.

Estimated nitrate breakthrough points for biochar amended soils were each within 0.5 pore volumes of the control (pore volume 11.4), indicating that biochar had little to no effect on the timing of nitrate release from HSL. The effect of biochar on the total quantity of nitrate released was also less substantial than for ammonium (Fig. 4b). Only SW500 significantly decreased the concentration of nitrate in the leachate compared to the control. At pore volume 15, SW500 inhibited nitrate transport by 35.01% ($p = 0.002$) (Fig. 5b). This effect was not present at pore volume 20, and was slightly lessened to 26.5% by pore volume 25 (marginally significant at $p = 0.098$).

https://doi.org/10.5194/soil-2021-45
Preprint. Discussion started: 27 May 2021

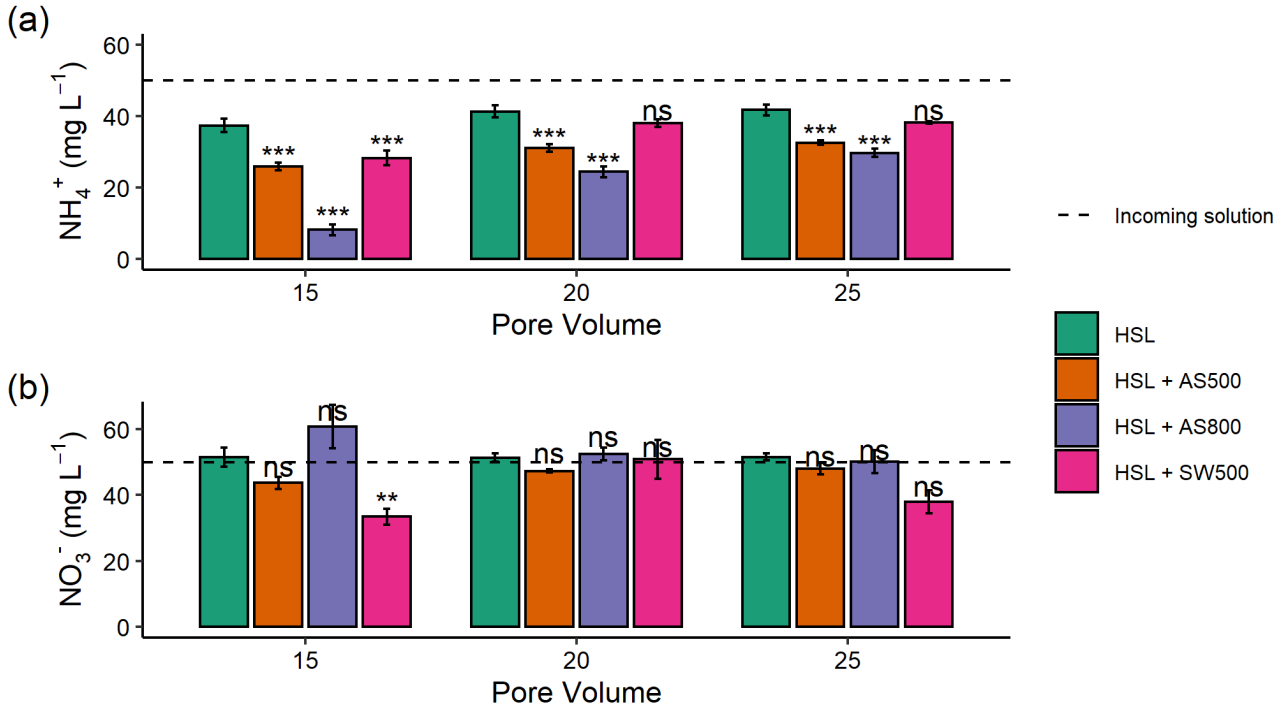

305 **Figure 5: Quantity of a) ammonium and b) nitrate in Hanford Sandy Loam (HSL) soil columns with 0 and 2% additions of AS500, AS800, and SW500 biochars in pore volumes 15, 20, and 25 (n=5). Error bars represent standard error of the means. Symbols denote significance levels as follows: ns = not significant, *p<0.05, **p<0.01, ***p<0.001. P-values refer to comparisons between treatments and the control within each pore volume, and were corrected for multiple comparisons using Tukey's honestly significant difference method.**

310

4 Discussion

4.1 Sorption and biochar properties

The ability of all seven biochars to retain ammonium, and within the demonstrated ranges, is consistent with other published studies (Zhang et al., 2020). AS800 exhibited substantially higher ammonium binding capacity than the other biochars tested.
315 While it is typical for biochars produced at high temperatures to have low O/C ratios and low CEC (Hassan et al., 2020), AS800 had the largest O/C ratio at 0.56 (presumably due to post-pyrolysis oxidation), and the second highest CEC at 52.75 cmolc kg^{-1}. These properties, as well as the IR band at 1405 cm^{-1}, likely explain the high ammonium retention, as they indicate increased exchange sites and oxygen-containing functional groups which can react with ammonium. The relationship between these biochar properties and ammonium binding capacity was also demonstrated with SW800, which had the highest CEC at

https://doi.org/10.5194/soil-2021-45
Preprint. Discussion started: 27 May 2021

60.83 cmolc kg^{-1}, the second highest O/C ratio at 0.27, and the second highest ammonium binding capacity. These observations are consistent with those of other studies (Gai et al., 2014a; Yang et al., 2017). No clear trends between surface area and ammonium retention emerged in this study.

That six of the seven biochars did not retain nitrate, and in most cases released nitrate, is consistent with other published studies (Zhang et al., 2020). Though data are inconclusive and show no clear trends to explain the chemical affinity between AS500 and nitrate, it is possible that the relatively high ash content and low CEC enabled anionic binding, as positively charged ions from biochar ash could bind to nitrate without being repelled by surface cation exchange sites. While AS800 and SW800 had higher ash contents, they also had substantially larger CECs. Electrostatic repulsion, then, may have prevented binding between the positively charged metals in the ash and the aqueous nitrate.

4.2 Column experiment- nutrient retention

As in the sorption trials, AS800 retained the greatest quantity of ammonium in the column studies, followed by AS500 and SW500. This suggests that the chemical affinity between biochar and ammonium is the controlling factor on the flow of ammonium through biochar-amended soils. By contrast, the flow of nitrate appears to be dictated, though minor in effect, by physical means. Unlike in sorption trials, AS500 did not retain significant quantities of nitrate. This suggests a weak chemical affinity between AS500 and nitrate, in which nitrate is readily desorbed from AS500. SW500, however, significantly inhibited the flow of nitrate, despite not exhibiting chemical affinity in sorption trials. This suggests the physical retention mechanism known as nitrate capture, which is believed to be facilitated by increased surface area and porosity (Haider et al., 2016, 2020; Kameyama et al., 2012; Kammann et al., 2015). Indeed, SW500 had a substantially larger surface area than AS500 (93.5 compared to 54.7 $m^2 g^{-1}$). AS800, however, had an even greater surface area at 188.2 $m^2 g^{-1}$, but exhibited no capacity to retain nitrate. This may have been due to the formation of larger macropores in AS800 (Fig. 1b), which allowed water to move through the biochar more quickly and limited the flow of nitrate into micropores where it could be retained. The strong ammonium binding capacity and high CEC of AS800 suggests a strongly negatively charged surface. Electrostatic repulsion between AS800 and nitrate, therefore, may have prevented nitrate capture. Together with sorption results, these breakthrough curves add to a growing body of literature which suggests that biochar may have a strong role in decreasing ammonium mobility in soils, but is unlikely to do so for nitrate without chemical or physical modification (Zhang et al., 2020).

4.3 Column experiment- saturated hydraulic conductivity

AS500 and SW500 significantly decreased K_{sat} by 75% in HSL. AS800 also decreased K_{sat} in HSL, though to a lesser extent and without statistical significance. This effect is in agreement with the literature, which consistently demonstrates decreased K_{sat} in coarse textured soils after biochar amendment, and is hypothesized to be the result of increased surface area, microporosity, and tortuosity, which can slow the movement of water through soils (Blanco-Canqui, 2017). By contrast,

https://doi.org/10.5194/soil-2021-45
Preprint. Discussion started: 27 May 2021

biochar typically increases K_{sat} in fine textured soils due to decreased bulk density and an increase in total porosity and mean pore size (Blanco-Canqui, 2017). This is in agreement with the 98% increase in K_{sat} in YSiL after amendment with AS800, but contrasts with the 64 and 80% reduction after the addition of AS500 and SW500, respectively. AS500 and SW500 had substantially larger particle sizes and smaller surface areas than AS800. Though pore size was not quantitatively measured in this study, it is possible that the pores of AS500 and SW500 were small enough to decrease mean pore size in the coarse soil as in Devereux et al. (2013) but were not large or numerous enough to increase K_{sat} in a fine soil. By contrast, the collapse of the lacy carbon pores in the AS500 compared to AS800 lead to the formation of both additional small pores with greater surface area (confirmed by BET), and larger macro-pores (as visualized by X-ray microCT) in AS800. This may indicate an ability for AS800 to increase overall porosity, mean pore size, and pore connectivity in YSiL, as seen in other studies (Quin et al., 2014). Broadly, the ability of each biochar to substantially influence the movement of water through each soil underscores its effect on the physical composition of soils. This fact contributes to the hypothesis that nitrate capture may have occurred in the case of SW500.

5 Conclusion

This project contributes to the literature by investigating the combination of chemical and physical mechanisms through which biochar influences nutrient retention and hydraulic conductivity. Biochar was demonstrated to control the flow of ammonium primarily through chemical affinity. Ammonium retention was linked to biochar properties such as high CEC, high O/C ratios, and the presence of oxygen-containing surface functional groups. Nitrate transport was shown to be controlled, though slightly, through physical means. This effect could perhaps be optimized by producing biochars, like SW500, which minimize CEC but maximize surface area, to encourage the physical entrapment of nitrate. Biochar also had a large effect on saturated hydraulic conductivity, though this effect was not consistent across biochars and soils. Broadly, the results of this study suggest that biochar may increase the residence time of water in sandy soils and increase drainage in fine textured soils, though soil- and biochar- specific investigation is required.

This study demonstrates that biochar can provide a suite of agronomic benefits, from nutrient retention to improvements in soil-water dynamics for crop production. This may be particularly relevant for flooded agricultural systems such as rice, where ammonium is the primary source of N and water retention is a key parameter for success. Additional research and quantitative analysis at the micron and sub-micron scale is required to assess the influence of biochar on soil porosity and pore architecture. Field-scale investigation using these soils and biochars is also ongoing, in order to link the impact of biochar on hydraulic conductivity and nutrient leaching to its influence on crop yield and nutrient use efficiency.

https://doi.org/10.5194/soil-2021-45
Preprint. Discussion started: 27 May 2021

Author contribution

Funding acquisition was carried out by SJP. DLG, SJP, MAN, and DAR conceptualized and designed the experiments. SJP carried out FTIR analysis and data visualization. DAR captured and reconstructed microCT images. All other experiments were carried out by DLG, under the supervision of SJP and MAN. DLG and IA conducted formal analysis and data visualization. DLG prepared the manuscript, with equal contributions from all co-authors.

Competing interests

The authors declare they have no conflict of interest.

Acknowledgements

We are grateful to Cool Planet, Pacific Biochar, Karr Group Co., and Premier Mushroom for providing the biochars used in this study. We would like to thank Dula Parkinson for their assistance at the Lawrence Berkeley National Laboratory Advanced Light Source (ALS) Beamline 8.3.2 microtomography facility. We are grateful to Mike Marsh and the staff at Object Research Systems for providing a license to Dragonfly software and for the technical support in reconstructing and interpreting microCT images. Thank you also to the Davis R Users group for statistical and coding consultation, and to Tad Doane and Alex Barbour for laboratory support.

Financial support

This publication was made possible by funding from the California Department of Food and Agriculture Fertilizer Research and Education Program (16-0662-SA-0), the Almond Board of California (17-ParikhS-COC-01), and the United States Department of Agriculture (USDA), National Institute of Food and Agriculture (NIFA) through Hatch Formula Funding (CA 2076-H) and multistate regional project (W-3045). ALS is supported by the Director, Office of Science, Office of Basic Energy Science, of the US Department of Energy under contract no. DE-AC02- 05CH11231. Additionally, this research was supported by the UC Davis Dissertation Year Fellowship, a Henry A. Jastro Graduate Research Award, the Beatrice Oberly and S. Atwood McKeehan Fellowship, and the Foundation for Food and Agriculture Research Fellowship.

References

Ahmadvand, M., Soltani, J., Ebrahim, S., Garmdareh, H. and Varavipour, M.: The relationship between the characteristics of Biochar produced at different temperatures and its impact on the uptake of NO3--N, Environ. Heal. Eng. Manag. J., 5(2), 67–75, doi:10.15171/EHEM.2018.10, 2018.

Blanco-Canqui, H.: Biochar and Soil Physical Properties, Soil Sci. Soc. Am. J., 81(4), 687–711, doi:10.2136/sssaj2017.01.0017, 2017.

Bu, X., Xue, J., Zhao, C., Wu, Y. and Han, F.: Nutrient Leaching and Retention in Riparian Soils as Influenced by Rice Husk Biochar Addition, Soil Sci., 182(7), 1, doi:10.1097/ss.0000000000000217, 2017.

Chandra, S., Medha, I. and Bhattacharya, J.: Potassium-iron rice straw biochar composite for sorption of nitrate, phosphate, and ammonium ions in soil for timely and controlled release, Sci. Total Environ., 712, 136337, doi:10.1016/j.scitotenv.2019.136337, 2020.

Clough, T. J. and Condron, L. M.: Biochar and the Nitrogen Cycle: Introduction, J. Environ. Qual., 39(4), 1218, doi:10.2134/jeq2010.0204, 2010.

Devereux, R. C., Sturrock, C. J. and Mooney, S. J.: The effects of biochar on soil physical properties and winter wheat growth, Earth Environ. Sci. Trans. R. Soc. Edinburgh, 103(1), 13–18, doi:10.1017/S1755691012000011, 2013.

Doane, T. A. and Horwath, W. R.: Spectrophotometric determination of nitrate with a single reagent, Anal. Lett., doi:10.1081/AL-120024647, 2003.

Downie, A., Crosky, A. and Munroe, P.: Characteristics of biochar – physical and structural properties, Biochar Environ. Manag. - Sci. Technol., 89–108, doi:10.4324/9780203762264, 2009.

Gai, X., Wang, H., Liu, J., Zhai, L., Liu, S., Ren, T. and Liu, H.: Effects of feedstock and pyrolysis temperature on biochar adsorption of ammonium and nitrate, PLoS One, 9(12), 1–19, doi:10.1371/journal.pone.0113888, 2014a.

Gai, X., Wang, H., Liu, J., Zhai, L., Liu, S., Ren, T. and Liu, H.: Effects of Feedstock and Pyrolysis Temperature on Biochar Adsorption of Ammonium and Nitrate, PLoS One, 9(12), doi:10.1371/journal.pone.0113888, 2014b.

Gao, F., Xue, Y., Deng, P., Cheng, X. and Yang, K.: Removal of aqueous ammonium by biochars derived from agricultural residuals at different pyrolysis temperatures, Chem. Speciat. Bioavailab., 27(2), 92–97, doi:10.1080/09542299.2015.1087162, 2015.

Gaskin, J. W., Steiner, C., Harris, K., Das, K. C. and Bibens, B.: Effect of Low-Temperature Pyrolysis Conditions on Biochar for Agricultural Use, Trans. ASABE, 51(6), 2061–2069, doi:10.13031/2013.25409, 2008.

Glaser, B. and Lehr, V. I.: Biochar effects on phosphorus availability in agricultural soils: A meta-analysis, Sci. Rep., 9(1), 1–9, doi:10.1038/s41598-019-45693-z, 2019.

Glaser, B., Lehmann, J. and Zech, W.: Ameliorating physical and chemical properties of highly weathered soils in the tropics with charcoal - A review, Biol. Fertil. Soils, 35(4), 219–230, doi:10.1007/s00374-002-0466-4, 2002.

Glaser, B., Wiedner, K., Seelig, S., Schmidt, H. P. and Gerber, H.: Biochar organic fertilizers from natural resources as substitute for mineral fertilizers, Agron. Sustain. Dev., 35(2), 667–678, doi:10.1007/s13593-014-0251-4, 2015.

Griffin, D. E., Wang, D., Parikh, S. J. and Scow, K. M.: Short-lived effects of walnut shell biochar on soils and crop yields in a long-term field experiment, Agric. Ecosyst. Environ., 236, 21–29, doi:10.1016/j.agee.2016.11.002, 2017.

Gürsoy, D., De Carlo, F., Xiao, X. and Jacobsen, C.: TomoPy: A framework for the analysis of synchrotron tomographic data, J. Synchrotron Radiat., 21(5), 1188–1193, doi:10.1107/S1600577514013939, 2014.

Haider, G., Steffens, D., Müller, C. and Kammann, C. I.: Standard Extraction Methods May Underestimate Nitrate Stocks Captured by Field-Aged Biochar, J. Environ. Qual., 45(4), 1196–1204, doi:10.2134/jeq2015.10.0529, 2016.

https://doi.org/10.5194/soil-2021-45
Preprint. Discussion started: 27 May 2021

Haider, G., Joseph, S., Steffens, D., Müller, C., Taherymoosavi, S., Mitchell, D. and Kammann, C. I.: Mineral nitrogen captured in field-aged biochar is plant-available, Sci. Rep., 10(1), 1–12, doi:10.1038/s41598-020-70586-x, 2020.

Hale, S. E., Alling, V., Martinsen, V., Mulder, J., Breedveld, G. D. and Cornelissen, G.: The sorption and desorption of phosphate-P, ammonium-N and nitrate-N in cacao shell and corn cob biochars, Chemosphere, 91(11), 1612–1619, doi:10.1016/j.chemosphere.2012.12.057, 2013a.

Hale, S. E., Alling, V., Martinsen, V., Mulder, J., Breedveld, G. D. and Cornelissen, G.: The sorption and desorption of phosphate-P, ammonium-N and nitrate-N in cacao shell and corn cob biochars, Chemosphere, 91(11), 1612–1619, doi:10.1016/j.chemosphere.2012.12.057, 2013b.

Hassan, M., Liu, Y., Naidu, R., Parikh, S. J., Du, J., Qi, F. and Willett, I. R.: Influences of feedstock sources and pyrolysis temperature on the properties of biochar and functionality as adsorbents: A meta-analysis, Sci. Total Environ., 744, 140714, doi:10.1016/j.scitotenv.2020.140714, 2020.

Hestrin, R., Torres-Rojas, D., Dynes, J. J., Hook, J. M., Regier, T. Z., Gillespie, A. W., Smernik, R. J. and Lehmann, J.: Fire-derived organic matter retains ammonia through covalent bond formation, Nat. Commun., 10(1), 1–8, doi:10.1038/s41467-019-08401-z, 2019.

Hollister, C. C., Bisogni, J. J. and Lehmann, J.: Ammonium, Nitrate, and Phosphate Sorption to and Solute Leaching from Biochars Prepared from Corn Stover (Zea mays L.) and Oak Wood (Quercus spp.), J. Environ. Qual., 42(1), 137–144, doi:10.2134/jeq2012.0033, 2013.

International Biochar Initiative (IBI): Standardized Product Definition and Product Testing Guidelines for Biochar That Is Used in Soil, Int. Biochar Initiat., (November), 23, doi:http://www.biochar-international.org/characterizationstandard. 22, 2015.

ISO [International Organization for Standardization]: Determination of the specific surface area of solids by gas adsorption - BET method (ISO 9277:2010(E)), Ref. number ISO, doi:10.1007/s11367-011-0297-3, 2010.

Jeffery, S., Verheijen, F. G. A., van der Velde, M. and Bastos, A. C.: A quantitative review of the effects of biochar application to soils on crop productivity using meta-analysis, Agric. Ecosyst. Environ., 144(1), 175–187, doi:10.1016/j.agee.2011.08.015, 2011.

Jones, D. L., Rousk, J., Edwards-Jones, G., DeLuca, T. H. and Murphy, D. V.: Biochar-mediated changes in soil quality and plant growth in a three year field trial, Soil Biol. Biochem., 45, 113–124, doi:10.1016/j.soilbio.2011.10.012, 2012.

Kameyama, K., Miyamoto, T., Shiono, T. and Shinogi, Y.: Influence of Sugarcane Bagasse-derived Biochar Application on Nitrate Leaching in Calcaric Dark Red Soil, J. Environ. Qual., 41(4), 1131–1137, doi:10.2134/jeq2010.0453, 2012.

Kammann, C. I., Schmidt, H. P., Messerschmidt, N., Linsel, S., Steffens, D., Müller, C., Koyro, H. W., Conte, P. and Stephen, J.: Plant growth improvement mediated by nitrate capture in co-composted biochar, Sci. Rep., 5, 1–13, doi:10.1038/srep11080, 2015.

Lenth, R.: Emmeans: estimated marginal means, Aka Least-Squares Means., https://cran.r-project.org/package=emmeans, doi:https://CRAN.R-project.org/package=emmeans, 2019.

https://doi.org/10.5194/soil-2021-45
Preprint. Discussion started: 27 May 2021

Li, S., Barreto, V., Li, R., Chen, G. and Hsieh, Y. P.: Nitrogen retention of biochar derived from different feedstocks at variable pyrolysis temperatures, J. Anal. Appl. Pyrolysis, 133, 136–146, doi:10.1016/j.jaap.2018.04.010, 2018.

Lim, T. J., Spokas, K. A., Feyereisen, G. and Novak, J. M.: Predicting the impact of biochar additions on soil hydraulic properties, Chemosphere, 142, 136–144, doi:10.1016/j.chemosphere.2015.06.069, 2016.

Martos, S., Mattana, S., Ribas, A., Albanell, E. and Domene, X.: Biochar application as a win-win strategy to mitigate soil nitrate pollution without compromising crop yields: a case study in a Mediterranean calcareous soil, J. Soils Sediments, 20(1), 220–233, doi:10.1007/s11368-019-02400-9, 2020.

Mukome, F. N. D., Zhang, X., Silva, L. C. R., Six, J. and Parikh, S. J.: Use of chemical and physical characteristics to investigate trends in biochar feedstocks, J. Agric. Food Chem., 61(9), 2196–2204, doi:10.1021/jf3049142, 2013.

Mulvaney, R. L., Yaremych, S. A., Khan, S. A., Swiader, J. M. and Horgan, B. P.: Use of Diffusion to Determine Soil Cation-Exchange Capacity by Ammonium Saturation, Commun. Soil Sci. Plant Anal., 35(1–2), 51–67, doi:10.1081/CSS-120027634, 2004.

Pandolfi, R. J., Allan, D. B., Arenholz, E., Barroso-Luque, L., Campbell, S. I., Caswell, T. A., Blair, A., De Carlo, F., Fackler, S., Fournier, A. P., Freychet, G., Fukuto, M., Gürsoy, D., Jiang, Z., Krishnan, H., Kumar, D., Kline, R. J., Li, R., Liman, C., Marchesini, S., Mehta, A., N'Diaye, A. T., Parkinson, D. Y., Parks, H., Pellouchoud, L. A., Perciano, T., Ren, F., Sahoo, S., Strzalka, J., Sunday, D., Tassone, C. J., Ushizima, D., Venkatakrishnan, S., Yager, K. G., Zwart, P., Sethian, J. A. and Hexemer, A.: Xi-cam: a versatile interface for data visualization and analysis, J. Synchrotron Radiat., 25(4), 1261–1270, doi:10.1107/S1600577518005787, 2018.

Paramashivam, D., Clough, T. J., Dickinson, N. M., Horswell, J., Lense, O., Clucas, L. and Robinson, B. H.: Effect of Pine Waste and Pine Biochar on Nitrogen Mobility in Biosolids, J. Environ. Qual., 45(1), 360–367, doi:10.2134/jeq2015.06.0298, 2016.

Parikh, S. J., Goyne, K. W., Margenot, A. J., Mukome, F. N. D. and Calderón, F. J.: Soil chemical insights provided through vibrational spectroscopy., 2014.

Pratiwi, E. P. A., Hillary, A. K., Fukuda, T. and Shinogi, Y.: The effects of rice husk char on ammonium, nitrate and phosphate retention and leaching in loamy soil, Geoderma, 277, 61–68, doi:10.1016/j.geoderma.2016.05.006, 2016.

Quin, P. R., Cowie, A. L., Flavel, R. J., Keen, B. P., Macdonald, L. M., Morris, S. G., Singh, B. P., Young, I. M. and Van Zwieten, L.: Oil mallee biochar improves soil structural properties-A study with x-ray micro-CT, Agric. Ecosyst. Environ., 191, 142–149, doi:10.1016/j.agee.2014.03.022, 2014.

R Core Team: R: A language and environment for statistical computing, [online] Available from: https://www.r-project.org/, 2020.

Sanford, J. R., Larson, R. A. and Runge, T.: Nitrate sorption to biochar following chemical oxidation, Sci. Total Environ., 669, 938–947, doi:10.1016/j.scitotenv.2019.03.061, 2019.

Sheldrick, B. H. and Wang, C.: Particle Size Distribution, Lewis Publications/CRC Press, Boca Raton, FL., 1993.

Soil Survey Staff: Web Soil Survey, Natural Resources Conservation Service, United States Department of Agriculture, Nat.

https://doi.org/10.5194/soil-2021-45
Preprint. Discussion started: 27 May 2021

Resour. Conserv. Serv. United States Dep. Agric., 1–2 [online] Available from: http://websoilsurvey.nrcs.usda.gov/ (Accessed 1 January 2021), 2014.

Song, H., Wang, J., Garg, A., Lin, X., Zheng, Q. and Sharma, S.: Potential of novel biochars produced from invasive aquatic species outside food chain in removing ammonium nitrogen: Comparison with conventional biochars and clinoptilolite, Sustain., 11(24), 1–18, doi:10.3390/su11247136, 2019.

Teutscherova, N., Houska, J., Navas, M., Masaguer, A., Benito, M. and Vazquez, E.: Leaching of ammonium and nitrate from Acrisol and Calcisol amended with holm oak biochar: A column study, Geoderma, 323, 136–145, doi:10.1016/j.geoderma.2018.03.004, 2018.

Thomas, C. W.: Soil pH and soil activity in Methods of Soil Analysis: Part 3 Chemical Methods, edited by D. L. Sparks, A. L. Page, P. A. Helmke, R. H. Loeppert, P. N. Soltanpour, M. A. Tabatabai, C. T. Johnston, and M. E. Summer, American Society of Agronomy Inc.; Soil Science Society of America, Madison, WI., 1996.

Tian, J., Miller, V., Chiu, P. C., Maresca, J. A., Guo, M. and Imhoff, P. T.: Nutrient release and ammonium sorption by poultry litter and wood biochars in stormwater treatment, Sci. Total Environ., 553, 596–606, doi:10.1016/j.scitotenv.2016.02.129, 2016.

US Patent and Trademark Office: Patent Application Full Text and Image Database, Pat. Appl. Full Text Image Database [online] Available from: http://appft.uspto.gov/netacgi/nph-Parser?Sect1=PTO2&Sect2=HITOFF&p=1&u=%2Fnetahtml%2FPTO%2Fsearch-bool.html&r=0&f=S&l=50&TERM1=biochar&FIELD1=&co1=AND&TERM2=&FIELD2=&d=PG01 (Accessed 20 August 2020), 2021.

Uttran, A., Loh, S. K., Kong, S. H. and Bachmann, R. T.: ADSORPTION OF NPK FERTILISER AND HUMIC ACID ON PALM KERNEL SHELL BIOCHAR, J. OIL PALM Res., 30(3), 472–484, doi:10.21894/jopr.2018.0029, 2018.

Verdouw, H., Van Echteld, C. J. A. and Dekkers, E. M. J.: Ammonia determination based on indophenol formation with sodium salicylate, Water Res., doi:10.1016/0043-1354(78)90107-0, 1978.

Wang, B., Lehmann, J., Hanley, K., Hestrin, R. and Enders, A.: Adsorption and desorption of ammonium by maple wood biochar as a function of oxidation and pH, Chemosphere, 138, 120–126, doi:10.1016/j.chemosphere.2015.05.062, 2015.

Wang, B., Yang, D.-Y. and Li, F.-Y.: REMOVAL OF NITRATE AND PHOSPHATE BY IMMOBILIZED BIOCHARS PREPARED FROM REEDS AND HEMATITE, FRESENIUS Environ. Bull., 26(7), 4825–4833, 2017.

Watanabe, F. S. and Olsen, S. R.: Test of an Ascorbic Acid Method for Determining Phosphorus in Water and NaHCO 3 Extracts from Soil , Soil Sci. Soc. Am. J., 29(6), doi:10.2136/sssaj1965.03615995002900060025x, 1965.

Web of Science: Core Collection Database, "Biochar," [online] Available from: http://apps.webofknowledge.com, 2020.

Wickham, H.: ggplot2: Elegant Graphics for Data Analysis, Springer-Verlag New York [online] Available from: https://ggplot2.tidyverse.org, 2016.

Wickham, H., Averick, M., Bryan, J., Chang, W., McGowan, L., François, R., Grolemund, G., Hayes, A., Henry, L., Hester, J., Kuhn, M., Pedersen, T., Miller, E., Bache, S., Müller, K., Ooms, J., Robinson, D., Seidel, D., Spinu, V., Takahashi, K.,

https://doi.org/10.5194/soil-2021-45
Preprint. Discussion started: 27 May 2021

Vaughan, D., Wilke, C., Woo, K. and Yutani, H.: Welcome to the Tidyverse, J. Open Source Softw., 4(43), 1686, doi:10.21105/joss.01686, 2019.

Yang, H. I., Lou, K., Rajapaksha, A. U., Ok, Y. S., Anyia, A. O. and Chang, S. X.: Adsorption of ammonium in aqueous solutions by pine sawdust and wheat straw biochars, Environ. Sci. Pollut. Res., 25(26), 25638–25647, doi:10.1007/s11356-017-8551-2, 2017.

Yao, Y., Gao, B., Zhang, M., Inyang, M. and Zimmerman, A. R.: Effect of biochar amendment on sorption and leaching of nitrate, ammonium, and phosphate in a sandy soil, Chemosphere, 89(11), 1467–1471, doi:10.1016/j.chemosphere.2012.06.002, 2012.

Yin, Q., Zhang, B., Wang, R. and Zhao, Z.: Phosphate and ammonium adsorption of sesame straw biochars produced at different pyrolysis temperatures, Environ. Sci. Pollut. Res., 25(5), 4320–4329, doi:10.1007/s11356-017-0778-4, 2018.

Yin, Q., Liu, M. and Ren, H.: Removal of Ammonium and Phosphate from Water by Mg-modified Biochar: Influence of Mg pretreatment and Pyrolysis Temperature, BIORESOURCES, 14(3), 6203–6218, doi:10.15376/biores.14.3.6203-6218, 2019.

Zeng, Z., Zhang, S., Li, T., Zhao, F., He, Z., Zhao, H., Yang, X., Wang, H., Zhao, J. and Rafiq, M. T.: Sorption of ammonium and phosphate from aqueous solution by biochar derived from phytoremediation plants, J. ZHEJIANG Univ. B, 14(12), 1152–1161, doi:10.1631/jzus.B1300102, 2013.

Zhang, D., Yan, M., Niu, Y., Liu, X., van Zwieten, L., Chen, D., Bian, R., Cheng, K., Li, L., Joseph, S., Zheng, J., Zhang, X., Zheng, J., Crowley, D., Filley, T. R. and Pan, G.: Is current biochar research addressing global soil constraints for sustainable agriculture?, Agric. Ecosyst. Environ., 226, 25–32, doi:10.1016/j.agee.2016.04.010, 2016.

Zhang, H., Voroney, R. P. and Price, G. W.: Effects of Temperature and Activation on Biochar Chemical Properties and Their Impact on Ammonium, Nitrate, and Phosphate Sorption, J. Environ. Qual., 46(4), 889–896, doi:10.2134/jeq2017.02.0043, 2017.

Zhang, M., Song, G., Gelardi, D. L., Huang, L., Khan, E., Parikh, S. J., Ok, Y. S., Song, G., Gelardi, D. L., Huang, L., Khan, E., Parikh, S. J. and Ok, Y. S.: Evaluating biochar and its modifications for the removal of ammonium, nitrate, and phosphate in water, Water Res., Preprint, doi:10.1016/j.watres.2020.116303, 2020.

Zheng, H., Wang, Z., Deng, X., Zhao, J., Luo, Y., Novak, J., Herbert, S. and Xing, B.: Characteristics and nutrient values of biochars produced from giant reed at different temperatures, Bioresour. Technol., 130, 463–471, doi:10.1016/j.biortech.2012.12.044, 2013.

Zhou, L., Xu, D., Li, Y., Pan, Q., Wang, J., Xue, L. and Howard, A.: Phosphorus and Nitrogen Adsorption Capacities of Biochars Derived from Feedstocks at Different Pyrolysis Temperatures, WATER, 11(8), doi:10.3390/w11081559, 2019.